Tellus (1984), *36A*, 490–504

A review of the Southern Oscillation: oceanic-atmospheric circulation changes and related rainfall anomalies

By VERNON E. KOUSKY[1], MARY T. KAGANO and IRACEMA F. A. CAVALCANTI, *Instituto de Pesquisas Espaciais—INPE Conselho Nacional de Desenvolvimento Cientifico e Technologico, CNPQ, 12.200—São José dos Campos, SP, Brazil*

(Manuscript received October 19, 1983; in final form March 14, 1984)

ABSTRACT

In this review of the Southern Oscillation we consider oceanic and atmospheric circulation changes and related rainfall anomalies with special emphasis on the region of South America. The climate anomalies associated with Southern Oscillation—El Niño (ENSO) events are highly persistent and nearly global in extent. The persistent nature of these events derives from strong coupling between atmosphere and ocean. Although the initial causes of the oscillation are unclear, once initiated the Southern Oscillation (SO) follows a certain sequence of events with well-defined effects on rainfall over a large portion of the tropics and subtropics. Drought in Australia, Indonesia, India, West Africa and Northeast Brazil as well as excessive rainfall in the central and eastern Pacific, Peru, Ecuador and Southern Brazil are all related to the SO. ENSO events are also associated with dramatic changes in the tropospheric flow pattern over a broad area of both hemispheres. Wintertime upper tropospheric subtropical jets are especially pronounced as are changes in the low level trade wind regime of both the South Pacific and South Atlantic Oceans. Mid-latitude blocking patterns are also more frequent in certain regions during ENSO events.

1. Introduction

Extreme climatic anomalies, such as prolonged drought and excessive rainfall, have a dramatic impact on the economies as well as the lives of the inhabitants of afflicted regions. Undoubtedly, the human suffering is the single most important aspect attributable to these anomalies. In some instances, the economic effects of extreme climatic events may have far reaching consequences, especially in developing countries which are greatly dependent on agriculture, such as India, Brazil and certain African states.

The meteorologist cannot hope to modify anomalous climatic events. However, he may contribute to minimizing the effects that such events have on the general population through improved forecasts based on a better physical understanding of the anomalies. Indeed, large scale climatic anomalies associated with drought or flood conditions offer the meteorologist the best opportunity for improved long range forecasts. This is due to the highly persistent nature of these anomalies which may, in some instances, last for periods up to several months.

In this paper, we review the atmospheric and oceanic anomalies associated with a very persistent climatic fluctuation—the Southern Oscillation. Although not periodic, this oscillation frequently follows a certain sequence of events with well-defined effects on rainfall over a large portion of the tropics and subtropics. We do not intend to present here a comprehensive review of previous works on this subject. Rather, we will present the salient characteristics of the oscillation with emphasis on the Southern Hemisphere. For a more comprehensive picture of the Southern Oscillation the reader is referred to some of the excellent papers recently written on the subject (e.g. Julian and

[1] Present affiliation: Department of Meteorology, University of Utah, Salt Lake City, Utah, 84112, USA.

Chervin, 1978; Horel and Wallace, 1981; Rasmusson and Carpenter, 1982; Philander, 1983; Rasmusson and Wallace, 1983).

2. The pressure seesaw between the Indian and Pacific Oceans

As early as the turn of this century studies indicated the existence of a pressure seesaw between Buenos Aires, Argentina and Sydney, Australia (see Rasmusson and Carpenter, 1982 for a discussion of these early works). Walker (1923, 1924, 1928a) and Walker and Bliss (1932, 1937) documented the characteristics and extent of this pressure oscillation and gave it the name Southern Oscillation (SO). Walker and Bliss (1932) noted that when the pressure is high over the Pacific it tends to be low in the eastern Indian Ocean–Indonesia region with greater than normal precipitation in the latter area.

Fig. 1 shows a time series of mean station level pressure in December–February for Tahiti and Darwin, Australia. The locations of these stations and others often referred to in the literature as being key stations in the SO are shown in Fig. 2 along with the mean SLP distribution. It is evident from Fig. 1 that the pressure at the two stations is highly negatively correlated.

In order to map the spatial extent of the SO, Berlage and de Boer (1959) and Berlage (1966) correlated SLP anomalies at Djakarta, Indonesia with SLP anomalies at selected stations over the entire globe. The same procedure was also applied,

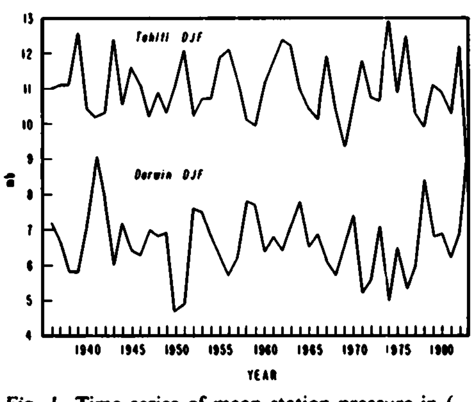

Fig. 1. Time series of mean station pressure in (−1000 mb) December–February at Tahiti and Darwin, Australia.

using Easter Island instead of Djakarta as the reference station (Berlage and de Boer, 1959). The results, using SLP anomalies at Easter Island[1] as the base series, are shown in Fig. 3 in the form of isolines of correlation coefficients. By comparing Figs. 2 and 3, it is apparent that there are two centers of action; one in the low pressure region of the eastern Indian Ocean near Indonesia and the other in the vicinity of the subtropical high in the central and eastern South Pacific.

The intensity and phase of the SO are often measured by means of indices. Most of these indices are computed by taking either a pressure difference or a difference in pressure deviations from normal between two stations which represent the two centers of action. The positive phase of the SO refers to the situation when both the Indonesian low pressure system and the East Pacific subtropical high are stronger than normal (e.g. when Tahiti SLP is higher than normal and Darwin SLP is lower than normal in Fig. 1). Under these conditions, surface convergence and related convective activity and precipitation are enhanced over the Indonesian region, due to stronger than normal southeast trade winds associated with the more intense subtropical high in the Pacific. Caviedes (1973) noted that for the positive phase of the SO (southeast trades stronger than normal) the Intertropical Convergence Zone (ITCZ) remains north of its normal position in the Eastern Pacific resulting in somewhat drier than normal conditions in that region.

During the negative phase of the SO, both the Indonesian low pressure system and the East Pacific subtropical high are weaker than normal. As a result, low level convergence and convective activity in Indonesia and northern Australia are less than normal. Due to the weaker subtropical high in the Pacific, the southeast trades are also weaker than normal thus permitting a more southward than normal displacement of the ITCZ in the

[1] The Easter Island series is relatively short, beginning in 1942 and, in the case of Fig. 3, extending through the late 1950's. Therefore, one should be cautious when discussing the level of the correlation coefficients analyzed in Fig. 3. However, the pattern in the South Pacific is quite similar to that shown in Fig. 1 of Trenberth (1976) and Fig. 10 of van Loon and Madden (1981), who used different reference stations and longer data records. Therefore, it is apparent that the overall pattern, in our Fig. 3, is correctly represented.

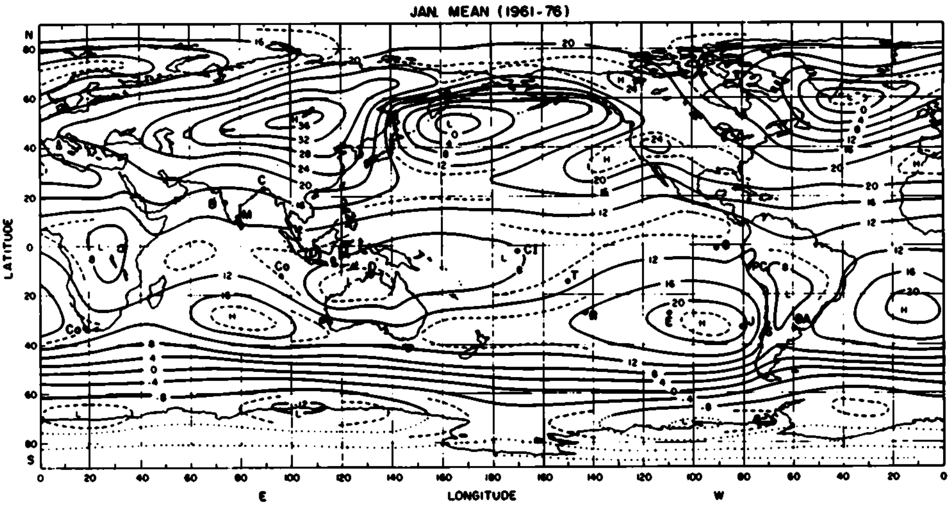

Fig. 2. January mean sea level pressure (1961–76). Adapted from Godbole and Shukla (1981). Stations commonly referred to as being key stations in the Southern Oscillation and indicated in the figure are: Capetown (Ca), Bombay (B), Madras (M), Calcutta (C), Djakarta (Dj), Darwin (D), Perth (P), Cocos Island (Co), Canton Island (CI), Papaete, Tahiti (T), Rapa (R), Easter Island (E), Juan Fernandez Island (J), Galapagos Islands (G), Puerto Chicama (PC), Santiago (S) and Buenos Aires (BA).

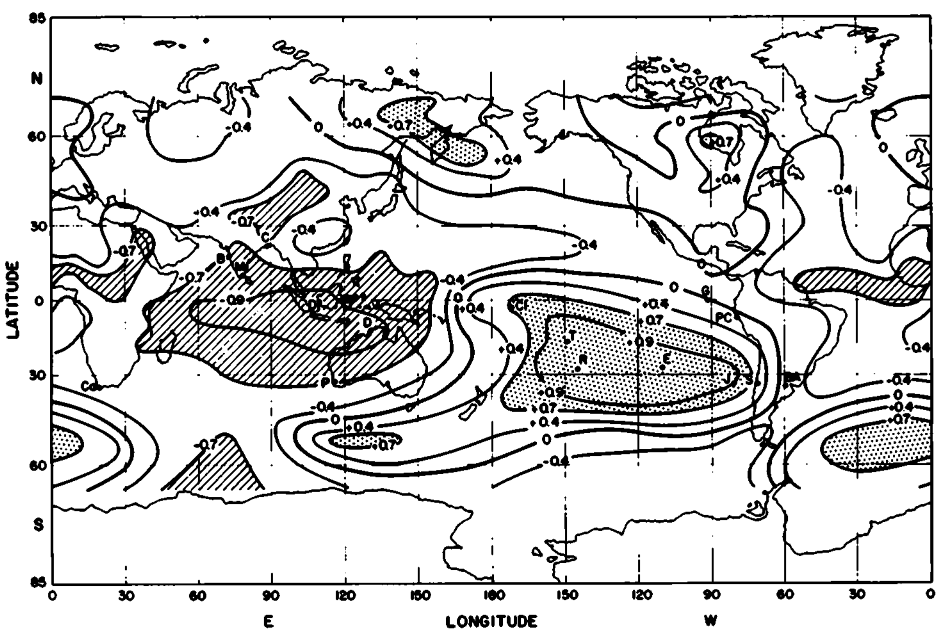

Fig. 3. Isolines of correlation coefficients of sea level pressure anomalies using Easter Island (E) as the reference station. Adapted from Berlage and de Boer (1959).

eastern Pacific with abnormally heavy rainfall in that region (Caviedes, 1973).

From the analysis shown in Fig. 3, Berlage and de Boer (1959) concluded that when the SO is strongly developed—either in its negative or positive phase—blocking action is stimulated at middle and high latitudes. Blocking is generally associated with anomalous low pressure at subtropical latitudes and high pressure at higher latitudes within the same longitudinal range. Evident in Fig. 3 are three regions where correlations substantially change sign with latitude in the Southern Hemisphere; (1) at the longitudes of the eastern Indian Ocean and Australia, (2) over the central and eastern South Pacific and (3) over the South Atlantic. These regions agree quite well with those found by van Loon (1956) to be preferred blocking areas.

During the positive phase of the SO both the Atlantic and Australian sectors have weaker than normal westerlies and SLP patterns similar to that for blocking situations. The Pacific region, on the other hand, has stronger than normal westerlies between 40 and 50° S. During the negative phase of the SO the situation is reversed, i.e. westerlies are weaker than normal suggesting that blocking is more frequent in the Pacific and westerlies are stronger than normal over the Atlantic and Australian sectors. Similar results concerning the relation between the Southern Hemisphere westerlies and the phases of the SO were obtained in a recent article by van Loon and Madden (1981). Since blocking occurs on a time scale considerably shorter than that of the data (annual average) used to construct Fig. 3, further study is necessary in order to confirm the relationship, if one exists, between Southern Hemisphere blocking and the phase of the SO.

3. Atmospheric–oceanic interactions

3.1. *Trade winds and ocean currents*

The locations of the main centers of action of the SO led Berlage and de Boer (1959) to conclude that the phenomenon is of maritime origin. This idea was pursued further by Troup (1965) who suggested that the southeast trades and their relation to sea surface temperature (SST) are important factors in initiating events.

On the average, the sea surface is relatively cold in the eastern equatorial Pacific and relatively warm in the western Pacific. This is primarily a result of the anticyclonic circulation in both the ocean and atmosphere in the Pacific region which results in relatively cold water being advected northward along the west coast of South America. Coastal upwelling, present along much of the Peruvian coast, contributes additional cold water that becomes part of the flow to very low latitudes. The Equatorial Current then carries this water westward across the Pacific. This zonal flow is gradually heated by solar radiation so that it is quite warm by the time it has arrived in the western Pacific. Thus, an east–west SST gradient is established in the equatorial Pacific. This gradient is enhanced, in a narrow region about the equator, due to equatorial upwelling in the eastern and central Pacific. This SST pattern is consistent with a thermally direct atmospheric circulation cell in which warm air rises over the western Pacific and relatively cool air sinks over the eastern Pacific, as depicted in Fig. 4.

Bjerknes (1969) gave the name "Walker Circulation" to this east–west convection cell. According to Bjerknes, weakening or strengthening of the Walker Circulation is associated with SST variations which tend to maintain this trend in intensity. This can be seen as follows. If the low level easterlies in the eastern and central Pacific were to weaken, then the SST's in the region would increase, due to reduced upwelling and a slowdown in the ocean currents, and the east–west temperature gradient would diminish, favoring a weaker Walker Circulation. On the other hand, if the low level easterlies were to strengthen, the SST's would decrease in the eastern equatorial Pacific, thus increasing the east–west temperature gradient and, consequently, a stronger Walker Circulation would be maintained.

The mechanism which causes either a weakening or strengthening of the southeast trades is not at all evident. It may be, as suggested by Wyrtki (1975), a more or less random forcing by the atmospheric circulation pattern at higher latitudes in the Southern Hemisphere. It is evident from past events that usually there is first a strengthening of the trades (strong Walker Circulation), then a rather sudden transition to the negative phase (weak Walker Circulation) of the SO. Wyrtki (1975) suggests that the intensification of the Walker Circulation causes an accumulation of

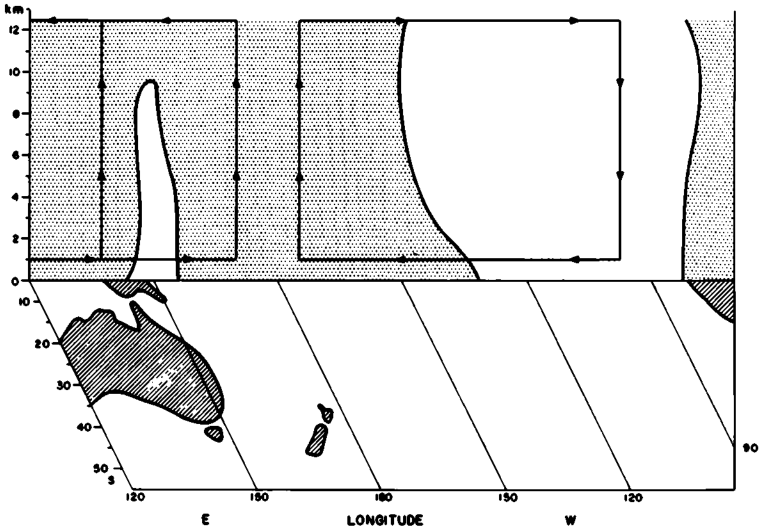

Fig. 4. Schematic diagram of the Pacific Walker Circulation. Shaded regions are areas of rising motion. The circulation pattern shown is the January mean for 1979–81 and is taken from Fig. 9.

warm water in the western Pacific. Once the trades weaken, the warm water is then transported eastward by ocean currents and by internal Kelvin waves which take about two months to travel from the western Pacific to the coast of Peru (Wyrtki, 1975, 1983). The response of the ocean to changes in the wind stress over the equatorial Pacific has recently been successfully simulated in a simple linear model by Busalacchi and O'Brien (1980).

3.2. *El Niño and its relation to the SO*

Every year around Christmas-time, the normally cold waters off the coast of Peru and near the coast of Ecuador give way to much warmer waters associated with a southward moving current called El Niño. This transition is often attributed to the ocean's response to the relaxation of the southeast trades, which are normally weakest during the southern summer (Bjerknes, 1966; Wooster and Guillén, 1974; Hickey, 1975).

In certain years the warming in this region is excessive and positive SST anomalies remain in the area for several months. An El Niño event is now commonly used to refer to this excessive warming and related atmospheric phenomena. Berlage (1966) demonstrated that the El Niño phenomenon is intimately linked to the SO by showing the remarkable similarity between the SLP curve for Darwin and the SST curve for Puerto Chicama, Peru. Similar results, shown in Fig. 5 for data up to 1982, have been obtained by Rasmusson and Wallace (1983), using Darwin SLP and central equatorial Pacific SST.

The tendency for El Niño events to occur during the southern summer indicates that the seasonal cycle plays an important role in the SO (Wyrtki, 1975). The build up of warm water in the western Pacific is greatly enhanced if, during a particular summer, the trade winds are stronger than normal. Thus, there would be 18 consecutive months of strong trades. As a result, when the trades finally weaken during the following summer, conditions would be favorable for an El Niño event. There is evidence that this is the most common sequence of events (Wyrtki, 1975).

4. The South Pacific convergence zone

Polar orbiting and geostationary meteorological satellites have contributed greatly in determining the main characteristics of global cloud distribution. Using data obtained from the polar orbiting ESSA satellites, Gruber (1972) identified brightness maxima associated with the ITCZ, located north of the equator in the Pacific, and a South Pacific Convergence Zone (SPCZ), which extends from New Guinea southeastward into the central

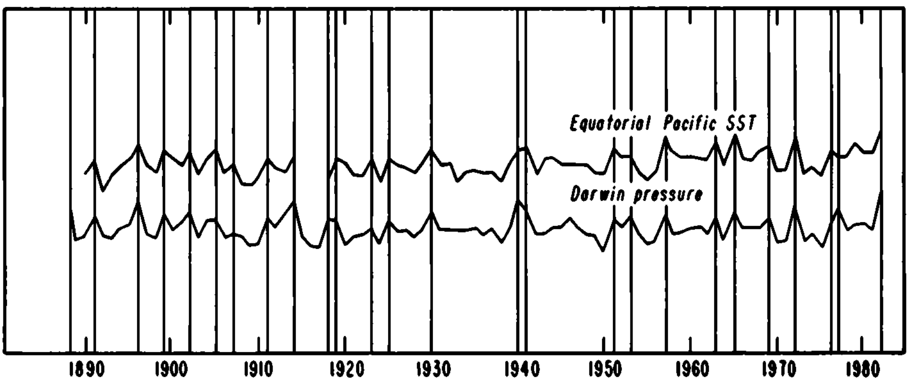

Fig. 5. Time series of equatorial eastern Pacific (South American coast to the dateline) sea surface temperature (April–March) and Darwin, Australia mean sea level pressure (April–March). Vertical lines indicate ENSO episodes. Adapted from Fig. 1 of Rasmusson and Wallace (1983). Printed by permission of *Science*, copyright 1983 by The American Association for the Advancement of Science.

South Pacific. Both of these features are evident in the 45 month mean outgoing long-wave radiation (OLW) pattern shown in Fig. 6.

A seasonasl shift in the position of the SPCZ is evident in the OLW data for the period 1974–1978 (Heddinghaus and Krueger, 1981; Liebmann and Hartmann, 1982). The SPCZ is farthest to the east (155° W, at 20° S) and most intense during the southern summer (December–February) and farthest to the west (175° E, at 20° S) during the southern winter (June–August) (Liebmann and Hartmann, 1982). This seasonality in the position of the SPCZ is linked to the seasonal cycles in the equatorial and eastern Pacific SST's and in the intensity of the central and eastern Pacific subtropical high.

Similar shifts in the SPCZ are found during the negative and positive phases of the SO (Trenberth, 1976). When the SO is in its positive phase (strong Walker Circulation), the SPCZ lies to the west of its mean position. This is in accord with above normal rainfall over Indonesia and eastern Australia and a stronger than normal subtropical high in the Pacific. When the SO is in its negative

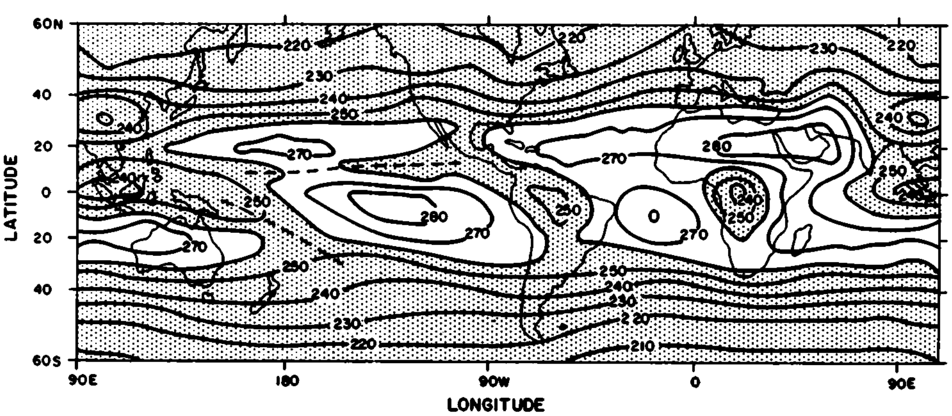

Fig. 6. Mean (June 1974 to February 1978) outgoing longwave radiation (OLW) pattern. Taken from an article in *Monthly Weather Review* by Heddinghaus and Krueger (1981). Printed by permission of the American Meteorological Society. Shaded areas have OLW values of less than 260 W m^{-2}. The ITCZ and SPCZ are indicated in dashed lines.

phase (weak Walker Circulation), the SPCZ lies east of its normal position, thus provoking above normal rainfall at many islands in the central Pacific. This agrees with a weaker than normal subtropical high and positive SST anomalies in the equatorial central and eastern Pacific.

The pattern of correlations associated with the SO (Fig. 3) extends well into the middle latitudes of the Southern Hemisphere. It is evident, therefore, that the mid-latitude westerlies are involved with the Walker Circulation and SPCZ (Trenberth, 1976). As mentioned previously, the correlation pattern in Fig. 3 suggests that blocking is more frequent at the longitudes of Australia during the positive phase of the SO, while during the negative phase, blocking is more frequent farther east in the central and eastern Pacific. Since the SPCZ shows this same displacement with the phases of the SO, it appears that the SPCZ plays an important role in midlatitude blocking in the above regions.

5. Teleconnections with extratropical latitudes

As evident from the preceding sections, the Southern Hemisphere midlatitude circulation is closely linked to the SO. Besides the work by Trenberth (1976), discussed in section 4, Bjerknes (1966, 1969, 1972), Horel and Wallace (1981), van Loon and Madden (1981), van Loon and Rogers (1981), Chen (1982) and Arkin (1982) have presented observational evidence of the SO teleconnections with circulation anomaly patterns at higher latitudes. Bjerknes (1966) suggested that the winter hemisphere Hadley cell is intensified during the negative (weak Walker Circulation) phase of the SO, when equatorial waters are anomalously warm in the central and eastern Pacific. The positive SST anomalies in this region tend to reduce (on rare occasions, reverse) the east–west gradient. With a more uniform SST in the equatorial Pacific, large scale convective overturning is favored in the meridional direction as opposed to the considerable east–west convective overturning that occurs during the positive phase of the SO. Presumably, this anomalous SST pattern leads to the anomalously strong subtropical jet streams observed during the respective winter seasons in both hemispheres (Arkin, 1982).

Horel and Wallace (1981) obtained an anomaly pattern which is qualitatively similar to the patterns presented by Bjerknes (1966, 1972) for warm episodes. This pattern, called the Pacific/North American (PNA) pattern, shows a series of alternating positive and negative geopotential height anomaly centers emanating from the tropical heat source region, first poleward then recurving eastward and eventually equatorward following a great circle route. Similar patterns have been obtained in the theoretical studies of Opsteegh and van den Dool (1980), Hoskins and Karoly (1981) and Webster (1981) who obtained steady state solutions of the linearized primitive equations on a sphere, forced by a tropical heat source. Similar patterns have also been obtained in general circulation model simulations in which equatorial Pacific SST anomalies, similar to those observed, have been imposed (Blackmon et al., 1983).

Simmons et al. (1983) have explored the role that barotropically unstable modes may have in producing the PNA pattern. Using a barotropic model, linearized about the 300 mb climatological mean January flow, initial perturbations were imposed at a variety of tropical and extratropical locations. Anomaly patterns resulted which are similar to the PNA pattern. Simmons et al., concluded that a great deal of the low frequency variability in the Northern Hemisphere wintertime circulation is due to barotropic instability where disturbances derive their energy from the basic state.

6. Rainfall anomalies associated with the SO

Walker (1923, 1924, 1928a) performed his worldwide correlation analyses in an attempt to provide forecast information concerning the Indian monsoon. Walker observed that, during the negative phase of the SO, rainfall in the region of Indonesia (including northern Australia) and India is below normal. Recent works by Bhalme et al. (1983) and Rasmusson and Carpenter (1983) confirm the tendency for extensive drought to occur in India during warm episodes, i.e. when SST's in the central Pacific are above normal. Warming of the SST's in the central Pacific usually follows warming along the Peruvian coast (El Niño) by up to six months (Rasmusson and Carpenter, 1983).

Recently, Quinn et al. (1978) showed that drought in Indonesia is also associated with El Niño. As discussed previously, rainfall in the central Pacific is above normal during the negative phase of the SO (warm episodes) (Trenberth, 1976; Horel and Wallace, 1981).

Recently, Streten (1983) showed that for a recent ENSO event, winter drought conditions were extensive in Australia. Streten's rainfall analyses, which include all of the Southern Hemisphere, show that the area of southern Brazil experienced abnormally wet conditions while Australia experienced drought. Mossman (1924) also noted the relation between the SO and rainfall over southern Brazil, Paraguay and northern Argentina, as represented by the level of the Parana river at Rosario, Argentina. Mossman's results, which agree with Streten's, show that positive river level departures occur during the negative phase of the SO, when SLP is anomalously high in the region of Australia. Fig. 7 shows the departures in the level of the Parana and a SO index (SOI) used by Berlage (1966). The two curves are remarkably alike with a correlation coefficient of 0.56 between the two series.

Walker (1928b) considered that anomalous rainfall in northeast Brazil is also related to the SO. Walker even developed a statistical regression scheme for drought prediction for that region. More recently, Caviedes (1973) and Hastenrath and Heller (1977) showed that drought in Northeast Brazil is related to El Niño events.

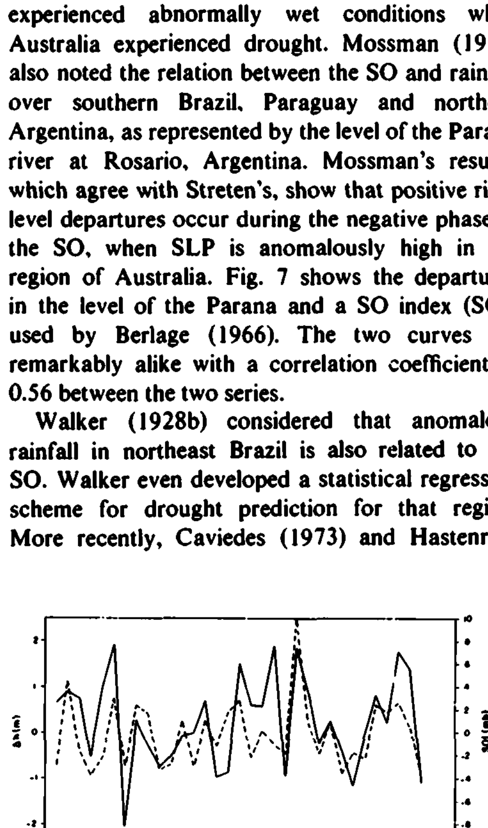

Fig. 7. The mean Parana river level anomalies (m), for April–September, at Rosario, Argentina (dashed line) and a Southern Oscillation Index (SOI) (solid line) calculated by taking the sum of the pressure anomalies (mb) at Bombay, Madras, Djakarta, Calcutta, Darwin, Perth and Cape Town for the period of October–March. The SOI values are plotted in the year corresponding to the January–March period, and are taken from Berlage (1966). The Parana river level anomalies are taken from Mossman (1924).

Berlage (1966) noted a high positive correlation between precipitation at Luanda, Angola (West Africa) and precipitation in the northern Northeast Brazil. Berlage also noted that the SO is directly involved in the rainfall anomalies in both regions. Recently, Moura and Kagano (1983) noted a similar correlation in rainfall between the two regions.

Fig. 8 has been constructed from data presented in the works of Rasmusson and Carpenter (1983), Quinn et al. (1978), Berlage (1966) and Bhalme et al. (1983), plus rainfall for 12 stations in Northeast Brazil (see Table 1 for the names and locations of these stations). Evident in this figure is a strong tendency for El Niño to occur simultaneously with or within one year of drought in northeast Brazil. The SOI shows a similar relationship to Northeast Brazil rainfall. Since the SOI, used here, is the sum of October–March SLP anomalies at several stations within the Australasia–Indian Ocean region, positive values correspond to the negative phase of the SO. Of the six highest peaks in the SOI, five are associated with either simultaneous drought in northeast Brazil or drought the following year. Since these five droughts (1915, 1919, 1932, 1942, 1958) are the severest, during the period presented in Fig. 8, it is evident that monitoring the SLP anomalies in the Australasia–Indian Ocean region may be useful in forecasting severe drought in northeast Brazil.

As noted by Berlage (1966) and also evident in Fig. 8, there is a positive correlation between rainfall at Luanda, Angola and precipitation in northeast Brazil. The correlation coefficient between the two series is 0.43, which is significant at greater than 99% level. The correlation coefficient between the SOI and northeast Brazil rainfall is −0.32, which, although lower in absolute value than that obtained between Luanda and the northeast, is still significant at greater than the 95% level. Such a low correlation, explaining only about 10% of the variance, indicates that the relation between rainfall in northeast Brazil and the SO is not an exceptionally strong one. But, as indicated by the previous discussion concerning the severest droughts and their relation to the peaks in the SOI, seasonal forecasts may be feasible if one is only concerned with extreme events. Fig. 8 also illustrates that drought in Indonesia and India are also linked to

Table 1. *Names and locations of stations used in preparing the time series of average percent of normal rainfall, presented in Fig. 8 for northeast Brazil.*

Station	State	Latitude (S)	Longitude (W)
Quixeramobim	Ceara	5°12′	39°19′
Crateu	Ceara	5°11′	40°40′
Saboeiro	Ceara	6°32′	39°54′
Milagres	Ceara	7°19′	38°57′
Augusto Severo	Rio Grande do Norte	5°51′	37°19′
Patu	Rio Grande do Norte	6°6′	37°38′
Cajazeiras	Paraiba	6°53′	38°34′
Pianco	Paraiba	7°11′	37°57′
Flores	Pernambuco	7°50′	37°59′
Sta. Maria da Boa Vista	Pernambuco	8°48′	39°50′
Casa Nova	Bahia	9°24′	41°8′
Remanso	Bahia	9°41′	42°4′

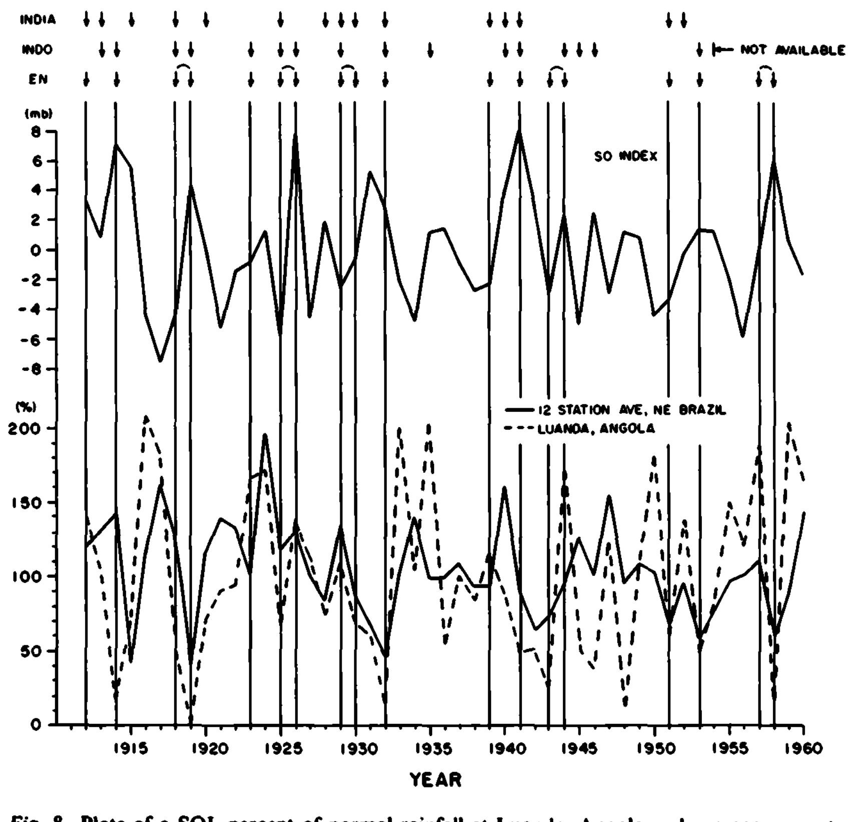

Fig. 8. Plots of a SOI, percent of normal rainfall at Luanda, Angola and average percent of normal rainfall for 12 stations in northeast Brazil for the period of 1912–60. Arrows at top of figure refer to El Niño events (two years events are connected by arcs) and drought in India and Indonesia. Indonesian drought and El Niño events taken from Quinn et al. (1978), India drought taken from Rasmusson and Carpenter (1983). The SOI is from Berlage (1966) as described in Fig. 7. Northeast Brazil stations are listed in Table 1. Luanda, Angola rainfall data are taken from Berlage (1966).

the SO, although as in the case of northeast Brazil this is not always the case. Droughts may be due to a number of causes ranging from regional atmospheric circulation anomalies to the global anomalies associated with the SO. The strongest ENSO events are clearly linked to severe drought in certain regions of the tropics and subtropics and excessive rainfall in others.

7. Atmospheric circulation patterns in the vicinity of South America

Kidson (1975), in his principal component or empirical orthogonal function (EOF) analysis of tropical SLP and rainfall, noted that the first eigenvector of SLP anomalies has a pattern similar to the correlation pattern of the SO. Aside from the usual centers of action, Kidson found another center of action over northern Brazil, particularly during the period December–February. This center he attributed to a Walker Circulation in the region of South America and the South Atlantic, during the southern summer. Newell (1979) also considered the existence of a Walker Circulation in this region.

Using the National Meteorological Center (NMC) tropical grid point data, we have computed the January mean mass adjusted kinematic vertical motions in pressure coordinates for the period 1979–1981, a period in which the SO indices indicate that the SO was neither in its positive nor in its negative phase (Arkin et al., 1983). These are presented in Fig. 9. The Pacific portion of this diagram was used to produce Fig. 4. In Fig. 9, we show the vertical motion and zonal wind component fields as a function of longitude and height at 5° S, as well as the basic horizontal flow characteristic near sea level (1000 mb) over oceanic areas. The SPCZ is evident in the Pacific as a region of cyclonic flow extending from 170° E–180° E, at 5° S, southeastward to about 150° W, at 30° S. Other important features are the cyclonic circulation near Australia and the anticyclonic circulations over the eastern Pacific and central Atlantic.

We have discussed the Pacific Walker Circulation previously. Focusing our attention now on the region of South America, we observe, in Fig. 9, general rising motion over the continent with sinking motion over the Atlantic and near the coast of Northeast Brazil. The zonal wind circulation is similar to that for the Pacific Walker Circulation, i.e. relatively strong low level easterlies and upper level westerlies in the region of sinking motion and fairly weak low and upper level flow in the vicinity of the rising motion.

Kidson (1975) suggests that the east–west Walker Circulation over Brazil and the South Atlantic is related to the SO in the same way as the Pacific Walker Circulation, i.e. these circulations are weak during the ENSO events. The weak Walker Circulation in the Pacific results from a reduced east–west temperature gradient due to

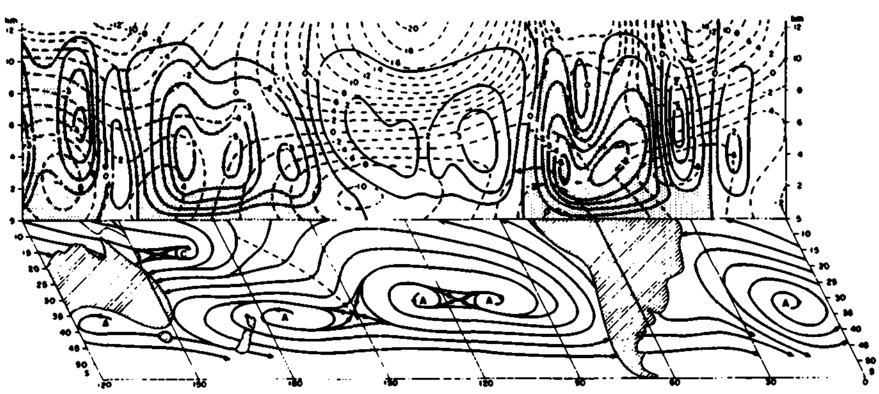

Fig. 9. Three dimensional diagram illustrating the January mean (1979–1981) 1000 mb streamline pattern (horizontal portion of diagram), vertical motion, w (solid lines, in units of 10^{-4} mb s^{-1}, with regions of upward motion shaded) and zonal wind (dashed lines), at 5° S, Fig. 4 is a schematic representation of the Pacific portion of this diagram. The SPCZ is indicated by the heavy dashed line in the 1000 mb streamline flow

anomalously warm SST's in the central and eastern Pacific. As a result of the more uniformly warm water in the equatorial Pacific, a stronger than normal Hadley Circulation exists, as suggested by Bjerknes (1966). This creates stronger than normal subtropical jets in both hemispheres with the winter hemisphere having the strongest jet. In the Southern Hemisphere, during summer, normal features such as the upper tropospheric anticyclones over South America and Australia and the Pacific mid-oceanic trough are presumably weaker during ENSO events with a tendency toward more zonal flow at subtropical and middle latitudes. During the southern winter months of ENSO events, a strong subtropical jet prevails over the central and eastern South Pacific (Arkin, 1982), which is analogous to the abnormally intense wintertime subtropical jet that extends east-northeastward from the southeast North Pacific across northern Mexico to the gulf coast area of the United States. The presence of this jet may be, in part, responsible for above normal fall and winter rainfall in southern Brazil (discussed in the preceding section) just as the northern jet may be related to above normal precipitation over northern Mexico and the Gulf Coast states (Rasmusson and Wallace, 1983).

8. Some aspects of the 1982–83 ENSO event compared to previous events

The latest ENSO event evolved in an abnormal fashion with positive SST anomalies appearing first in the central Pacific, during the southern winter, instead of near the coast of South America, during the southern summer. Also, there was no apparent build-up in the strength of the southeast trades prior to the onset of the event. The disastrous effects that this event had on the rainfall distribution within the tropics and subtropics has been extensively covered by the news media. Clearly, this event was one of the strongest that has been recorded.

The Climate Analysis Center, in a series of special bulletins (Climate Analysis Center, 1983a, b, c, d), followed the complete evolution of the 1982–83 event. This event has also been discussed by Rasmusson and Hall (1983), Arkin et al. (1983) and Rasmusson and Wallace (1983). Although it began in a manner different from the composite ENSO event, as presented by Rasmusson and Carpenter (1982), many of its characteristics were similar to previous events. The rainfall pattern over Brazil, during the 1982–83 event, was similar to that for the warm events of 1972 and 1976. Table 2 gives the rainfall anomalies, for the three events, at selected stations in the Amazon Basin and northeast Brazil, while Table 3 gives the anomalies for stations in eastern and southern Brazil. Negative rainfall anomalies, during the period January–May, were recorded in the Amazon Basin and the Northeast during all three events, with the greatest deficiencies occurring during the 1982–83 event. On the other hand, excessive rainfall was recorded during the winter months for stations in southern and southeastern Brazil. The meridional position of the greatest positive anomalies is not the same for all three events, having been farthest south in 1972, farthest north in 1976 and in between those two positions for the latest event.

Table 2. *January–May rainfall anomalies (mm) for selected stations in the Amazon Basin and northeast parts of Brazil, during the last three ENSO events. The five-month normal rainfall (mm) is given in the last column on the right. *February, 1976 departure at Manaus is absent.*

	January–May			
Station	1972	1976	1983	Mean
Sao Gabriel do Cachoeira 0°8′ S, 67°5′ W	−6	−93	−407	1394
Manaus 3°7′ S, 60° 1′ W	−78	−19*	−416	1334
Belem 1°28′ S, 48°29′ W	−224	−168	−387	1808
Barra do Corda 5°30′ S, 45°16′ W	−92	−42	−133	796
Conceicao do Araguaia 8°16′ S, 49°17′ W	−189	−234	−178	978
Fortaleza 3°43′ S, 38°33′ W	−458	+102	−456	1146
Quixeramobim 5°12′ S, 39°18′ W	−151	−39	−291	563

Table 3. *June–August rainfall anomalies (mm) for selected stations in eastern and southern Brazil, during the last three ENSO events. The three-month normal rainfall (mm) is given in the last column on the right.*

	June–August			
Station	1972	1976	1983	Mean
Caravelas 17°44′ S, 39° 15′ W	−178	+46	−89	313
Rio de Janeiro 22°54′ S, 43° 10′ W	+4	+143	+99	128
Sao Paulo 23°30′ S, 46°37′ W	+63	+260	+179	106
Curitiba 25°26′ S, 49° 14′ W	+35	+9	+244	253
Porto Alegre 30°5′ S, 51° 11′ W	+296	+80	+167	382

Associated with the anomalously warm sea surface in the central and eastern Pacific, the upper tropospheric circulation pattern exhibited stronger than normal subtropical jets in the respective winter hemispheres, plus very prominent anticyclonic circulation anomalies on both sides of the equator in the central Pacific. These features are consistent with the warm episode composite presented by Arkin (1982). Stronger than normal 850 mb easterlies and 200 mb westerlies prevailed over the eastern Amazon Basin and equatorial Atlantic (Arkin et al., 1983). Stronger than normal 200 mb westerlies in this region are also a feature of the composite analysis of ENSO events presented by Arkin (1982).

This tropospheric circulation anomaly pattern, when compared to the pattern shown in Fig. 9, suggest a strong Walker-type circulation with upward motion over the anomalously warm waters of the central and eastern Pacific and sinking motion over the eastern Amazon, Northeast Brazil and the equatorial Atlantic. Assuming that this pattern is more or less representative of the stronger ENSO events, it becomes evident why strong El Niño events and severe Northeast Brazil drought are closely related. The increased strength of the trades in the Atlantic, during ENSO events, creates negative SST anomalies which, as shown by Hastenrath and Heller (1977), Markham and McLain (1977) and Moura and Shukla (1981), is an important characteristic of drought years in northeast Brazil. Negative SST anomalies in the south Atlantic are also positively correlated to drought in Angola, West Africa (Hirst and Hastenrath, 1983), which is consistent with Berlage's (1966) results linking drought in Angola to drought in northeast Brazil.

The strong Walker Circulation, described above, which is partly a westward displacement of the normal Atlantic Walker Circulation, is a different mechanism for northeast Brazil drought than that proposed by Moura and Shukla (1981). It is also different from the circulation pattern expected by Kidson (1975), i.e. a weak Atlantic Walker Circulation in El Niño years. However, the above scheme appears to be physically consistent in that it provides a plausible explanation of why severe drought in northeast Brazil, El Niño and drought in West Africa are all related.

9. Conclusion

The Southern Oscillation (SO) is clearly a highly persistent global phenomenon resulting from a strongly coupled ocean–atmosphere system. Although much progress has been made in documenting the characteristics and effects of the SO there still remains the question of how it is initiated. In this paper, we have presented some of the salient global characteristics of the SO with emphasis on those features related to climate variability in the Southern Hemisphere.

The usual ENSO event begins with a strengthening of the southeast trades in the Pacific and an accumulation of warm water in the western equatorial Pacific. The trades then weaken, usually during the southern summer, and the warm water is transported eastward across the equatorial Pacific. Thus, the normal east–west SST gradient is weakened and the normal Walker Circulation is greatly altered. Due to the zonally symmetric distribution of anomalously warm water in the equatorial Pacific, a stronger than normal Hadley Circulation is generated and, as a consequence, upper level subtropical jets are stronger and more persistent than normal in both hemispheres. The stronger Hadley Circulation favors an intensification of the trade winds, which in the Southern

Hemisphere are observed during the winter. The increased trades tend to restore the SST's to their pre-El Niño state, i.e. an SST pattern favoring a stronger Walker Circulation and weaker Hadley Circulation. Thus, the SO generally proceeds to its mature warm stage within 6–12 months after initiation, which usually occurs during the southern fall (April–June). Then, the ocean–atmosphere system takes an additional six months to return to its normal state. Therefore, sometime during the second summer of an ENSO event conditions return to near normal.

During the latest (1982–83) ENSO event, circulation features were observed by inspection of daily surface and upper charts and satellite images. We noted that, besides the very pronounced subtropical jet, several mid-latitude blocking events occurred in the vicinity of South America and the eastern Pacific. These events, in combination with the subtropical jet, favored the maintenance of persistent active frontal systems in southern Brazil and, thus, contributed to excessive rain which fell in that region. Further research is needed to determine if blocking in the South American region is a feature characteristic of ENSO events.

10. Acknowledgments

The authors wish to thank Dr. M. R. Stevenson for reviewing the manuscript and for providing useful reference material. Thanks also to Dr. A. D. Moura for many useful discussions prior to and during the preparation of this manuscript.

The first author wishes to thank Dr. Phillip Arkin for providing the data used in Fig. 1. The first draft was typed by Ms. Maria de Fatima S. Massunaga. The final version was typed by Miss Jennifer L. Marcus.

The final revision of this work was supported jointly by the National Science Foundation, the National Oceanic and Atmospheric Administration, and the National Aeronautics and Space Administration under Grant No. ATM 8219198.

REFERENCES

Arkin, P. A. 1982. The relationship between interannual variability in the 200 mb tropical wind field and the Southern Oscillation. *Mon. Wea. Rev. 110*, 1393–1404.

Arkin, P. A., Kopman, J. D. and Reynolds, R. W. 1983. 1982–1983 El Niño/Southern Oscillation Event quick look atlas (Available from NOAA/NWS Climate Analysis Center, National Meteorological Center, Washington, D.C., 20233).

Berlage, H. P. 1966. The Southern Oscillation and world weather. *Mededel. Verhandel. 88*, Kon. Ned. Meteor. Inst., 152 pp.

Berlage, H. P. and de Boer, H. J. 1959. On the extension of the Southern Oscillation throughout the world during the period July 1, 1949 up to July 1, 1957. *Geofis. pura e appl. 44*, 287–295.

Bhalme, H. N., Mooley, D. A. and Jadhav, S. K. 1983. Fluctuations in the Drought/flood area over India and relationships with the Southern Oscillation. *Mon. Wea. Rev. 111*, 86–94.

Bjerknes, J. 1966. A possible response of the atmospheric Hadley circulation to equatorial anomalies of ocean temperature. *Tellus 18*, 820–829.

Bjerknes, J. 1969. Atmospheric teleconnections from the equatorial Pacific. *Mon. Wea. Rev. 97*, 163–172.

Bjerknes, J. 1972. Large-scale atmospheric response to the 1965–65 Pacific equatorial warming. *J. Phys. Oceanogr. 2*, 212–217.

Blackmon, M. L., Geisler, J. E. and Pitcher, E. J. 1983. A general circulation model study of January climate anomaly patterns associated with interannual variation of equatorial Pacific sea surface temperature. *J. Atmos. Sci. 40*, 1410–1425.

Busalacchi, A. J. and O'Brien, J. J. 1980. The seasonal variability in a model of the tropical Pacific. *J. Phys. Oceanogr. 10*, 1929–1951.

Caviedes, C. N. 1973. Secas and El Niño: Two simulations climatical hazards in South America. *Proc. Assoc. Amer. Geogr. 5*, 44–49.

Chen, W. Y. 1982. Fluctuations in Northern Hemisphere 700 mb height field associated with the Southern Oscillation. *Mon. Wea. Rev. 110*, 808–823.

Climate Analysis Center 1983a. Special climate diagnostics bulletin, 14 February, 1983. Equatorial Pacific warm episode reaches mature state. (Available from NOAA/NWS Climate Analysis Center, National Meteorological Center, Washington, D.C., 20233.)

Climate Analysis Center 1983b. Special climate diagnostics bulletin, 15 April 1983. Update on the 1982–83 equatorial Pacific warm episode. (Available from NOAA/NWS Climate Analysis Centre, National Meteorological Center, Washington, D.C., 20233.)

Climate Analysis Center 1983c. Special Climate diagnostics bulletin, 15 June 1983. The 1982–83 Pacific warm episode: Intense El Niño conditions persists in eastern equatorial Pacific. (Available from NOAA/NWS, Climate Analysis Center, National Meteorological Center, Washington, D.C., 20233.)

Climate Analysis Center 1983d. Special climate diagnostic bulletin, 15 July 1983. The 1982–83 Pacific warm episode: Falling sea surface temperatures in the eastern equatorial Pacific. (Available from NOAA/NWS, Climate Analysis Center, National Meteorological Center, Washington, D.C., 20233.)

Godbole, R. V. and Shukla, J. 1981. Global analysis of January and July sea level pressure. NASA Technical Memorandum 82097, Goddard Space Flight Center, Greenbelt, Maryland, 20771.

Gruber, A. 1972. Fluctuations in the position of the ITCZ in the Atlantic and Pacific Oceans. *J. Atmos. Sci. 29*, 193–197.

Hastenrath, S. and Heller, L. 1977. Dynamics of climatic hazards in northeast Brazil. *Q. J. R. Meteorol. Soc. 103*, 77–92.

Heddinghaus, T. R. and Krueger, A. F. 1981. Annual and inter-annual variations in outgoing long-wave radiation over the tropics. *Mon. Wea. Rev. 109*, 1208–1218.

Hickey, B. 1975. The relationship between fluctuations in sea level, wind stress and sea surface temperature in the equatorial Pacific. *J. Phys. Oceanogr. 5*, 460–475.

Hirst, A. C. and Hastenrath, S. 1983. On mechanisms of sea temperature and rainfall anomalies in the Angola-tropical Atlantic sector. Preprints First International Conference on Southern Hemisphere Meteorology, 31 July–6 August 1983, São José dos Campos, Brazil, 130–131.

Horel, J. D. and Wallace, J. M. 1981. Planetary-scale atmospheric phenomena associated with the Southern Oscillation. *Mon. Wea. Rev. 109*, 813–829.

Hoskins, B. J. and Karoly, D. 1981. The steady linear response of a spherical atmosphere to thermal and orographic forcing. *J. Atmos. Sci. 38*, 1179–1196.

Julian, P. R. and Chervin, R. M. 1978. A study of the Southern Oscillation and Walker Circulation phenomenon. *Mon. Wea. Rev. 106*, 1433–1451.

Kidson, J. W. 1975. Tropical eigenvector analysis and the Southern Oscillation. *Mon. Wea. Rev. 103*, 187–196.

Liebmann, B. and Hartmann, D. L. 1982. Interannual variations of outgoing IR associated with tropical circulation changes during 1974–78. *J. Atmos. Sci. 39*, 1153–1162.

Markham, C. G. and McLain, D. R. 1977. Sea surface temperature related to rain in Ceara, northeast Brazil. *Nature 265*, 320–323.

Mossman, R. C. 1924. Indian monsoon rainfall in relation to South American weather, 1875–1914. *Mem. Ind. Meteorol. Dept. 23*, 157–242.

Moura, A. D. and Shukla, J. 1981. On the dynamics of drought in Northeast Brazil: Observations, theory and numerical experiments with a general circulation model. *J. Atmos. Sci. 38*, 2653–2675.

Moura, A. D. and Kagano, M. T. 1983. Teleconnections between South America and western Africa as revealed by monthly precipitation analyses. Preprints First International Conference on Southern Hemisphere Meteorology, 31 July–6 August 1983, São José dos Campos, Brazil, 120–122.

Newell, R. E. 1979. Climate and the ocean. *Amer. Sci. 67*, 405–416.

Opsteegh, J. D. and van den Dool, H. M. 1980. Seasonal differences in the stationary response of a linearized primitive equation model: Prospects for long-range forecasting? *J. Atmos. Sci. 37*, 2169–2185.

Philander, S. G. H. 1983. El Niño Southern Oscillation phenomena. *Nature 302*, 295–301.

Quinn, W. N., Zopf, D. O., Short, K. S. and Kuo Yang, R. T. W. 1978. Historical trends and statistics of the Southern Oscillation, El Niño, and Indonesian droughts. *Fish. Bull. 76*, 663–678.

Rasmusson, E. M. and Carpenter, T. H. 1982. Variations in tropical sea surface temperature and surface wind fields associated with the Southern Oscillation/El Niño. *Mon. Wea. Rev. 110*, 354–384.

Rasmusson, E. M. and Carpenter, T. H. 1983. The relationship between eastern equatorial Pacific sea surface temperatures and rainfall over India and Sri Lanka. *Mon. Wea. Rev. 111*, 517–528.

Rasmusson, E. M. and Wallace, J. M. 1983. Meteorological aspects of the El Niño/Southern Oscillation. *Science 222*, 1195–1202.

Rasmusson, E. M. and Hall, J. M. 1983. Pacific Ocean event of 1982–83. *Weatherwise 36*, 166–175.

Simmons, A. J., Wallace, J. M. and Branstator, G. W. 1983. Barotropic wave propagation and instability and atmospheric teleconnection patterns. *J. Atmos. Sci. 40*, 1363–1392.

Streten, N. A. 1983. Southern Hemisphere circulation contrasts in the winters of 1972 and 1973. Preprints First International Conference on Southern Hemisphere Meteorology, 31 July–6 August, 1983, São José dos Campos, Brazil, 108–111.

Trenberth, K. E. 1976. Spatial and temperal variations of the Southern Oscillation. *Q. J. R. Meteorol. Soc. 102*, 639–653.

Troup, A. J. 1965. The Southern Oscillation. *Q. J. R. Meteorol. Soc. 91*, 490–506.

van Loon, H. 1956. Blocking action in the Southern Hemisphere, Part I. *Notos 5*, 171–175.

van Loon, H. and Madden, R. A. 1981. The Southern Oscillation. Part 1: Global associations with pressure and temperature in northern winter. *Mon. Wea. Rev. 109*, 1150–1162.

van Loon, H. and Rogers, J. C. 1981. The Southern Oscillation. Part 2: Associations with changes in the middle troposphere in the northern winter. *Mon. Wea. Rev. 109*, 1163–1168.

Walker, G. T. 1923. Correlation in seasonal variations of weather VIII. *Mem. Ind. Meteorol. Dept. 24*, 75–131.

Walker, G. T. 1924: Correlation in seasonal variation of weather IX. *Mem. Ind. Meteorol. Dept. 24*, 275–332.

Walker, G. T. 1928a. World Weather III. *Mem. R. Meteorol. Soc. 2*, 97–106.

Walker, G. T. 1928b. Ceara (Brazil) famines and the general air movement. *Beith. Phys. d. freien Atmos. 14*, 88–93.

Walker, G. T. and Bliss, E. W. 1932. World Weather V. *Mem. R. Meteorol. Soc. 4*, 53–84.

Walker, G. T. and Bliss, E. W. 1937. World Weather IV. *Mem. R. Meteorol. Soc. 4*, 119–139.

Webster, P. J. 1981. Mechanisms determining the atmospheric response to sea surface temperature anomalies. *J. Atmos. Sci. 38*, 554–571.

Wooster, W. S. and Guillén, O. 1974. Characteristics of El Niño in 1972. *J. Mar. Res. 32*, 387–404.

Wyrtki, K. 1975. El Niño—The dynamic response of the equatorial Pacific Ocean to atmospheric forcing. *J. Phys. Oceanogr. 5*, 572–584.

Wyrtki, K. 1983. Sea level in the equatorial Pacific in 1982. Tropical Ocean. *Atmos. Newsl. No. 16*, 6–7.